Figures and figure supplements

Patient-specific iPSC-derived photoreceptor precursor cells as a means to investigate retinitis pigmentosa

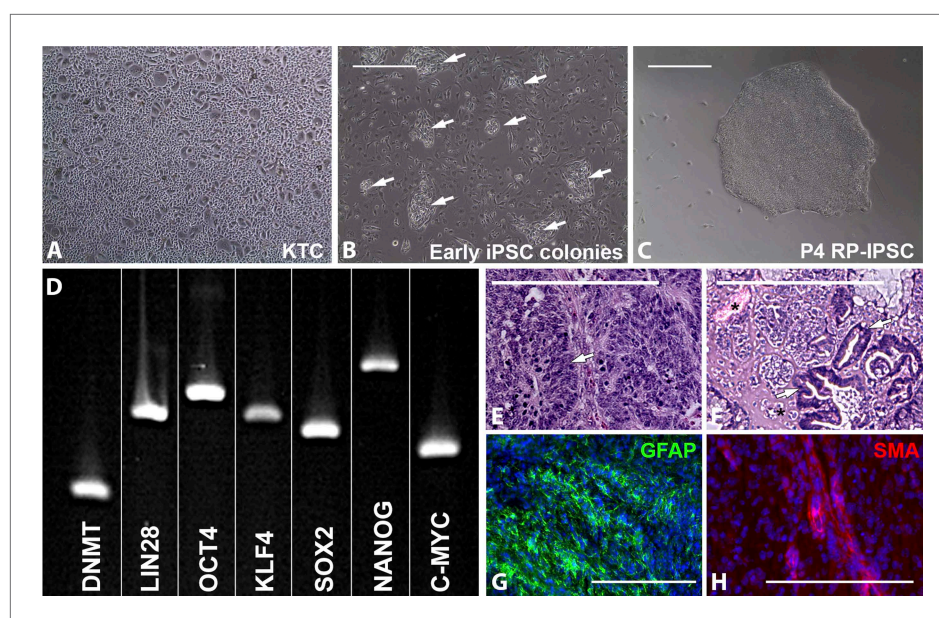**Budd A Tucker, et al.**

Figure 1. Derivation of iPSCs from keratinocytes of a patient affected with *USH2A*-associated RP. (**A–H**) Microscopic analysis of human keratinocytes (**A**), early keratinocyte-derived iPSC colonies (**B**, arrows), and purified keratinocyte-derived iPSC cultures (**C**). At 2–3 weeks post-viral transduction, ES-cell-like iPSC colonies begin to emerge (**B**, arrows). iPSC colonies isolated, subcultured, and expanded on Synthemax cell culture surfaces maintain a pluripotent morphology (**C**) express the pluripotency markers DNMT, LIN28, OCT4, KLF4, SOX2, NANOG, and C-MYC (**D**), and form teratomas consisting of tissues of ectoderm (**E**, arrow and **G**, GFAP in green), mesoderm (**F**, asterisk and **H**, SMA in red), and endoderm (**F**, arrows) each of the three embryonic germ layers (**E–H**). Scale bar = 400 µm.
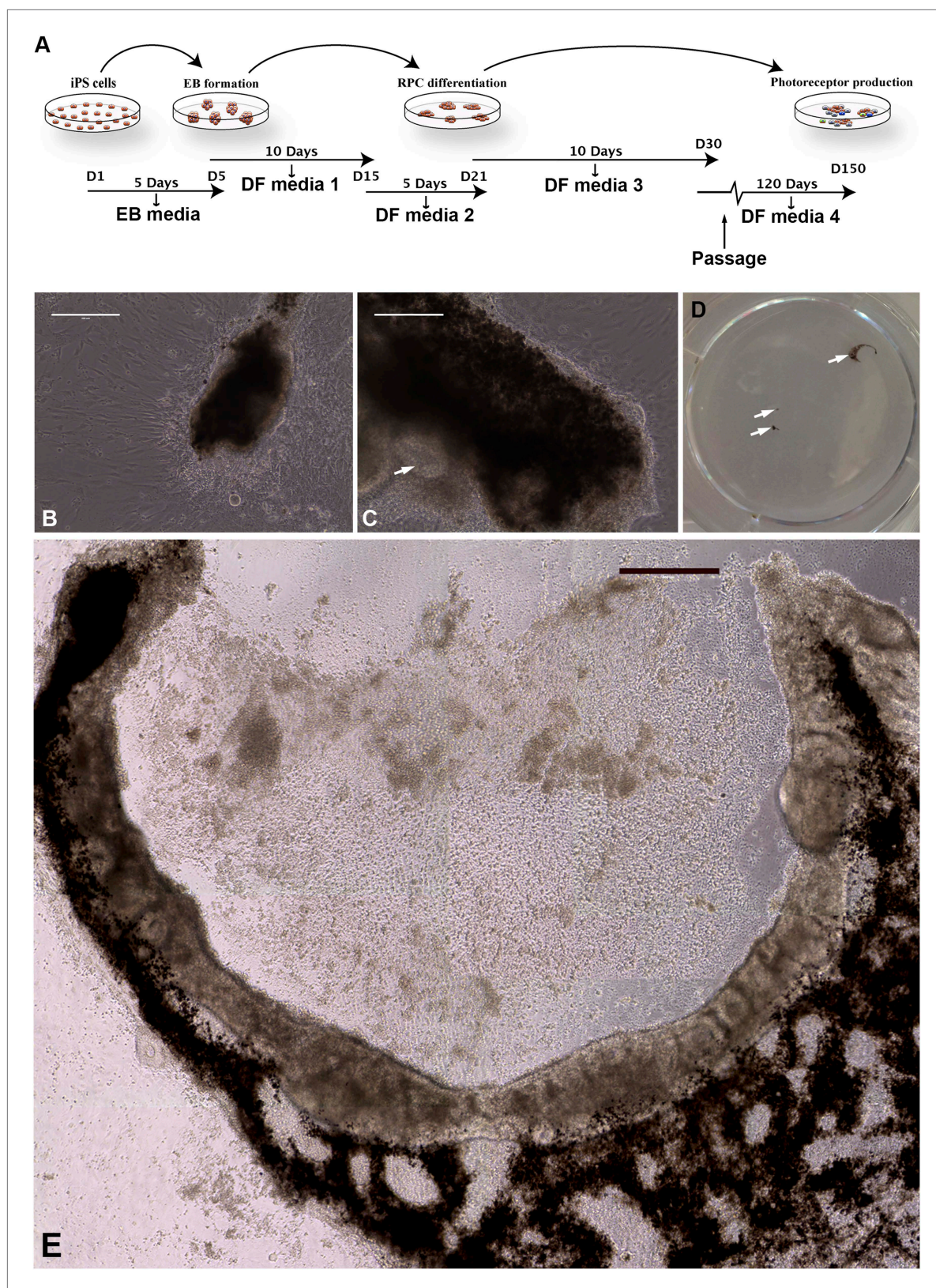DOI: 10.7554/eLife.00824.003

Figure 2. Differentiation of human *USH2A*-associated iPSCs into eyecup-like structures. (**A**) Schematic diagram illustrating the differentiation paradigm utilized to generate human eyecup-like structures. (**B**–**E**) Morphological analysis of *USH2A*-associated iPSC-derived eyecups. iPSC-derived eyecups form
Figure 2. Continued on next page

Figure 2. Continued

pigmented cell clumps (**B**) that extend and wrap in a C shape around newly formed neural rossettes (**C**). Following this protocol, a typical six-well cell culture dish will have two to four eyecups/well, each at slightly different stages of development (**D**, arrows, a low magnification image of a typical well of a six-well plate with developing eyecups). At 150 days post-differentiation, complete eyecups with clearly defined neural retina and RPE layers can be identified (**D**, top right arrow, and **E**). Scale bar, **B** and **C** = 200 μm, **D** = 400 μm.
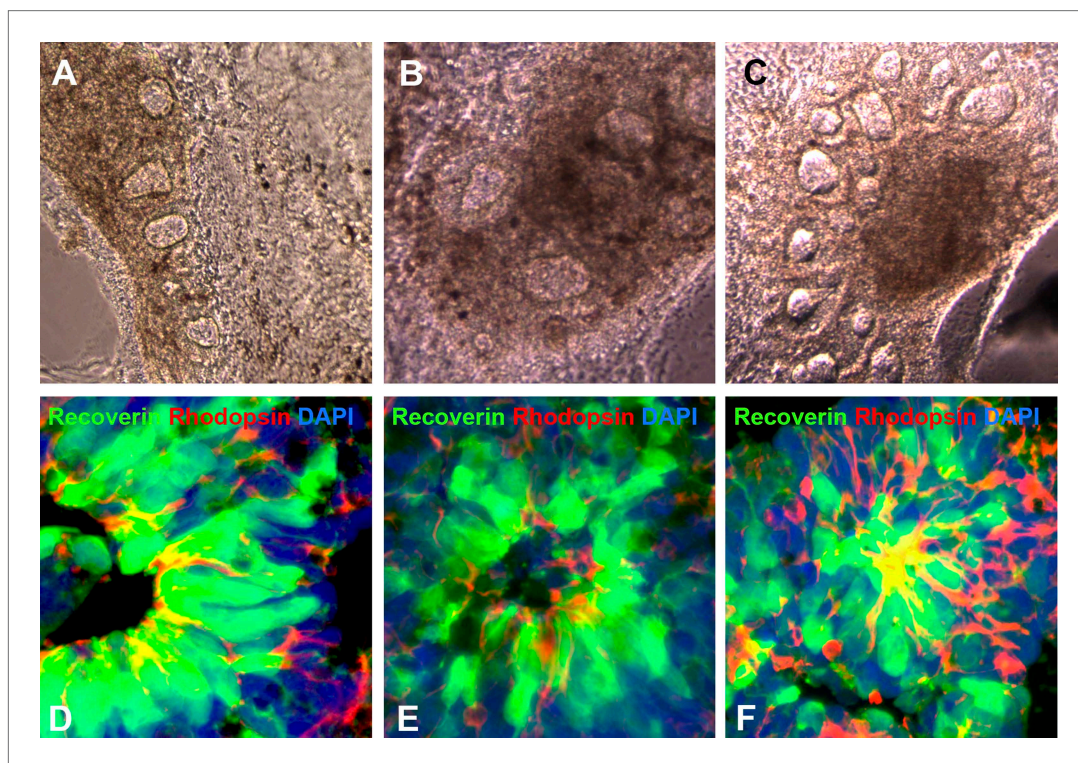
Figure 2—figure supplement 1. Additional examples of human *USH2A*-associated iPSC-derived eyecup-like structures. (**A–C**) At 150 days post-differentiation, extensive neural rosette formation was present. (**D–F**) Immunocytochemical analysis targeted against recoverin and rhodopsin confirms that neural rosettes consisted predominantly of rod photoreceptor precursor cells.
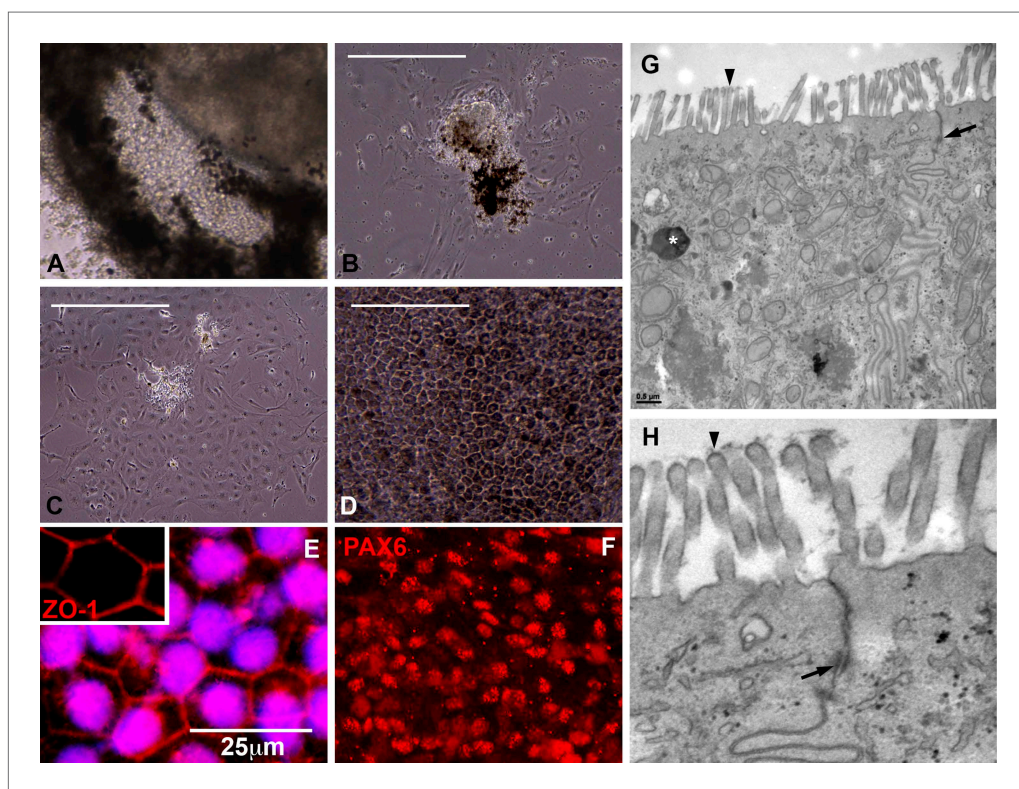
Figure 3. Cells contained within the pigmented layer of *USH2A*-associated eyecups are of RPE origin. (**A**) A high magnification phase image of the RPE layer of an *USH2A* eyecup prior to biopsy and subculture. (**B–D**) Area of the RPE presented in panel **A** was picked and subcultured in fresh RPE culture media on collagen, laminin, and fibronectin coated six-well culture dishes. 24 hr after plating, RPE cells spread and take on a fibroblastic morphology (**B**). By 72 hr post-plating, RPE cells lose their pigmentation and begin to form cell–cell contacts (**C**). 2 weeks post-plating, a confluent monolayer of RPE cells are present that have taken on the typical cuboidal RPE morphology and regained pigmentation (**D**). (**E–F**) Immunocytochemical analysis of *USH2A*-associated RPE cells with antibodies targeted against the tight junction marker ZO1 (**E**) and the transcription factor PAX6 (**F**). (**G–H**) TEM analysis of RPE cells within the intact RPE layer of *USH2A* eyecups (**H** is a high magnification view of the upper right corner of panel **G**). RPE cells are polarized, have apical microvilli, make tight junctions with neighboring RPE cells (**G** and **H**, arrows) and contain pigment granules within their cytoplasm (**G**, asterisk). Scale bar, **B–D** = 200 µm, **G** = 0.5 µm.
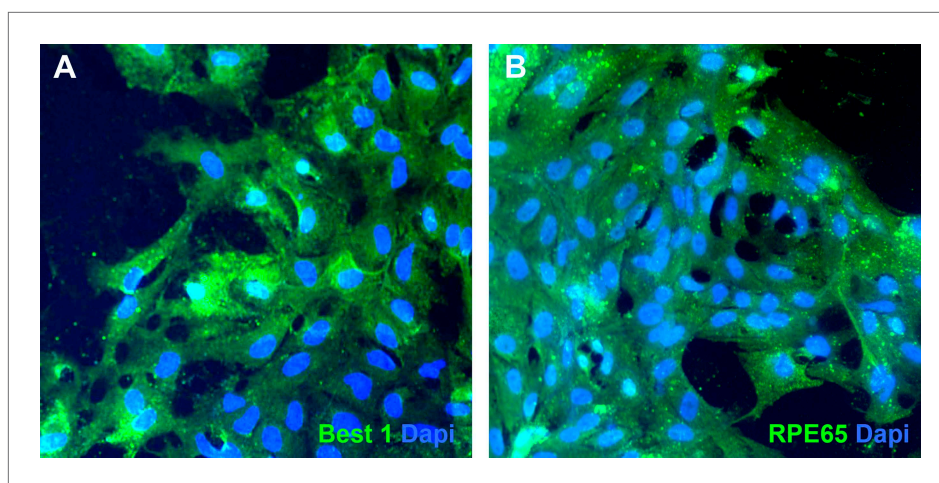DOI: 10.7554/eLife.00824.006

Figure 3—figure supplement 1. Pigmented cells isolated from *USH2A*-associated eyecups express bestrophin 1 and RPE65. (**A** and **B**) Immunocytochemical analysis of subcultured *USH2A*-associated RPE cells with antibodies targeted against bestrophin 1 (**A**) and RPE65 (**B**).
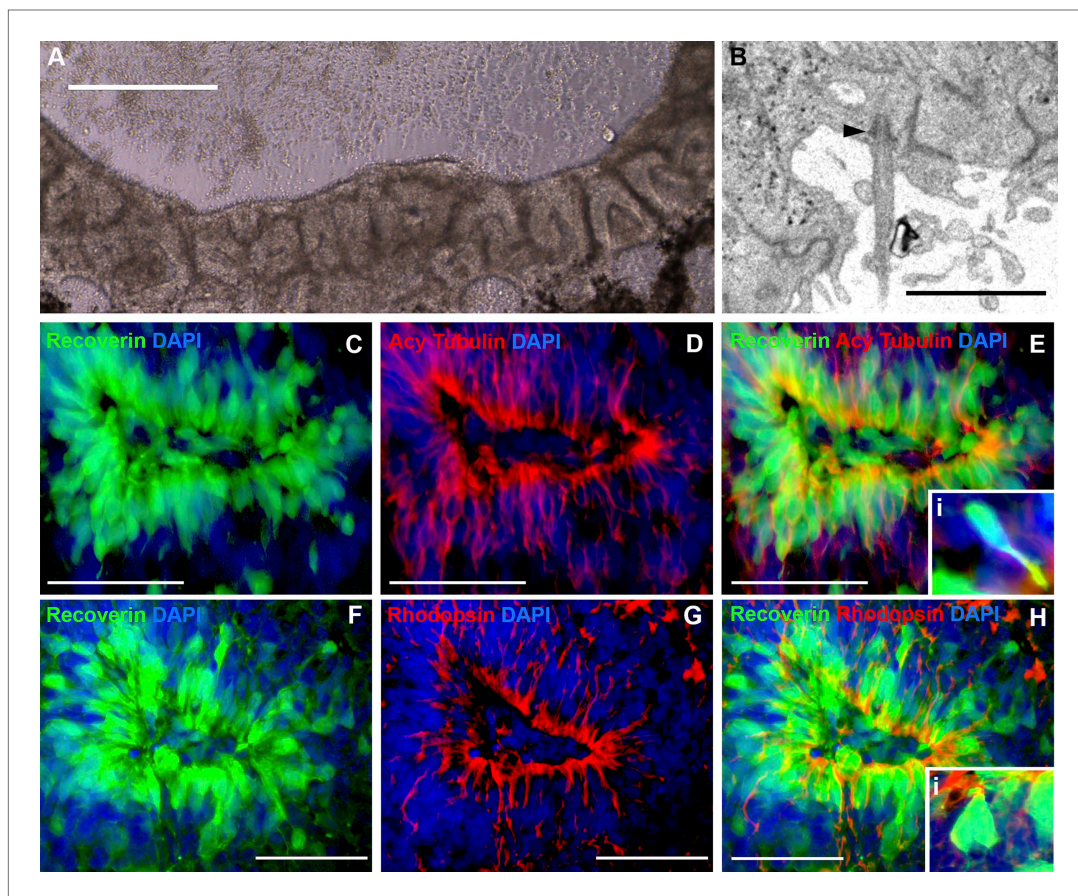DOI: 10.7554/eLife.00824.007

Figure 4. iPSC-derived USH2A-associated neural retinal rosettes consist predominantly of rod photoreceptor cells. (**A**) Morphological depiction of the neural retina at 120 days post-differentiation. (**B**) TEM analysis of neural rosettes demonstrates the existence of cilia with clearly identifiable basal bodies. (**C**–**H**) Immunocytochemical analysis targeted against the rod photoreceptor markers recoverin and rhodopsin (**C**–**E** and **Ei**-high magnification inlay), and the rod photoreceptor marker recoverin and the connecting cilia marker acetylated tubulin (**F**–**H** and **Hi**-high magnification inlay).
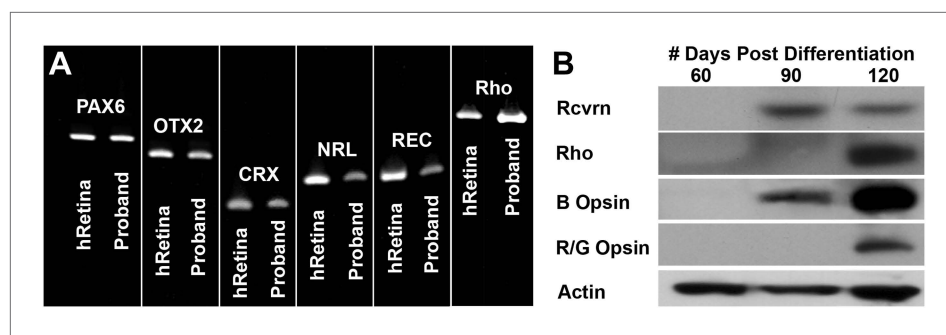DOI: 10.7554/eLife.00824.008

Figure 5. Developmental timeline of neural retina marker expression. (**A**) RT-PCR analysis of *USH2A* and human control neural retina for expression of the retinal transcription factors/photoreceptor markers PAX6, OTX2, CRX, NRL, recoverin, and rhodopsin at 60 days post-differentiation. (**B**) Western blot analysis of *USH2A* neural retina for expression of the retinal photoreceptor markers recoverin, rhodopsin, blue cone opsin and red/green cone opsin at 60, 90, and 120 days post-differentiation. Although retinal transcripts can be detected as early as 60 days post-differentiation, mature photoreceptor proteins such as recoverin, rhodopsin, and the cone opsins could not be detected until 90 to 120 days post-differentiation.
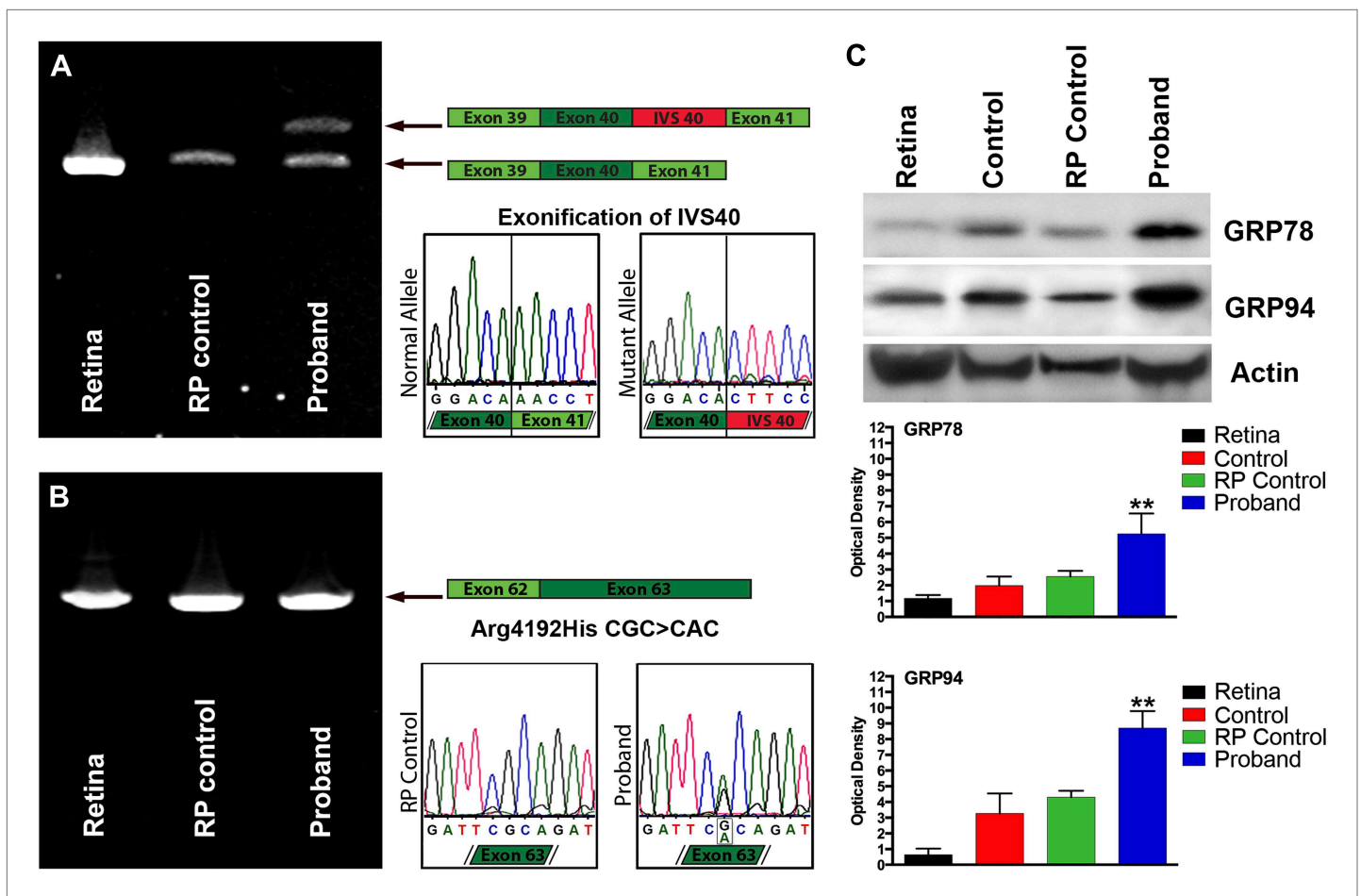DOI: 10.7554/eLife.00824.009

Figure 6. Confirmation of genomic *USH2A* variants in iPSC-derived neural retina. (**A**) RT-PCR analysis of USH2A exons 39 to 41 in human control retina (*DePristo et al., 2011*), human control iPSC-derived neural retina (*Baux et al., 2007*), and human RP iPSC-derived neural retina. An intronic splice site mutation in intervening sequence 40 of the USH2A gene results in the introduction of a pseudoexon (IVS40 Red) causing a translation frameshift and a premature stop codon. (**B**) RT-PCR analysis of *USH2A* exon 62 to 63 in human control human retina (*DePristo et al., 2011*), human control iPSC-derived neural retina (*Baux et al., 2007*), and human RP iPSC-derived neural retina. A single heterozygous point mutation identified by whole exome sequencing (Arg4192His) was confirmed in the proband's retinal transcript. (**C**) Western blot analysis of protein isolated from human control retina and iPSC-derived photoreceptor precursor cells obtained from the proband, an unaffected control, and a separate RP patient with known disease pathophysiology for expression of the ER-stress markers GRP78 and GRP94. Elevated expression of both GRP78 and GRP94 suggests that the mutations identified within the proband result in protein misfolding and ER-stress. **p<0.001
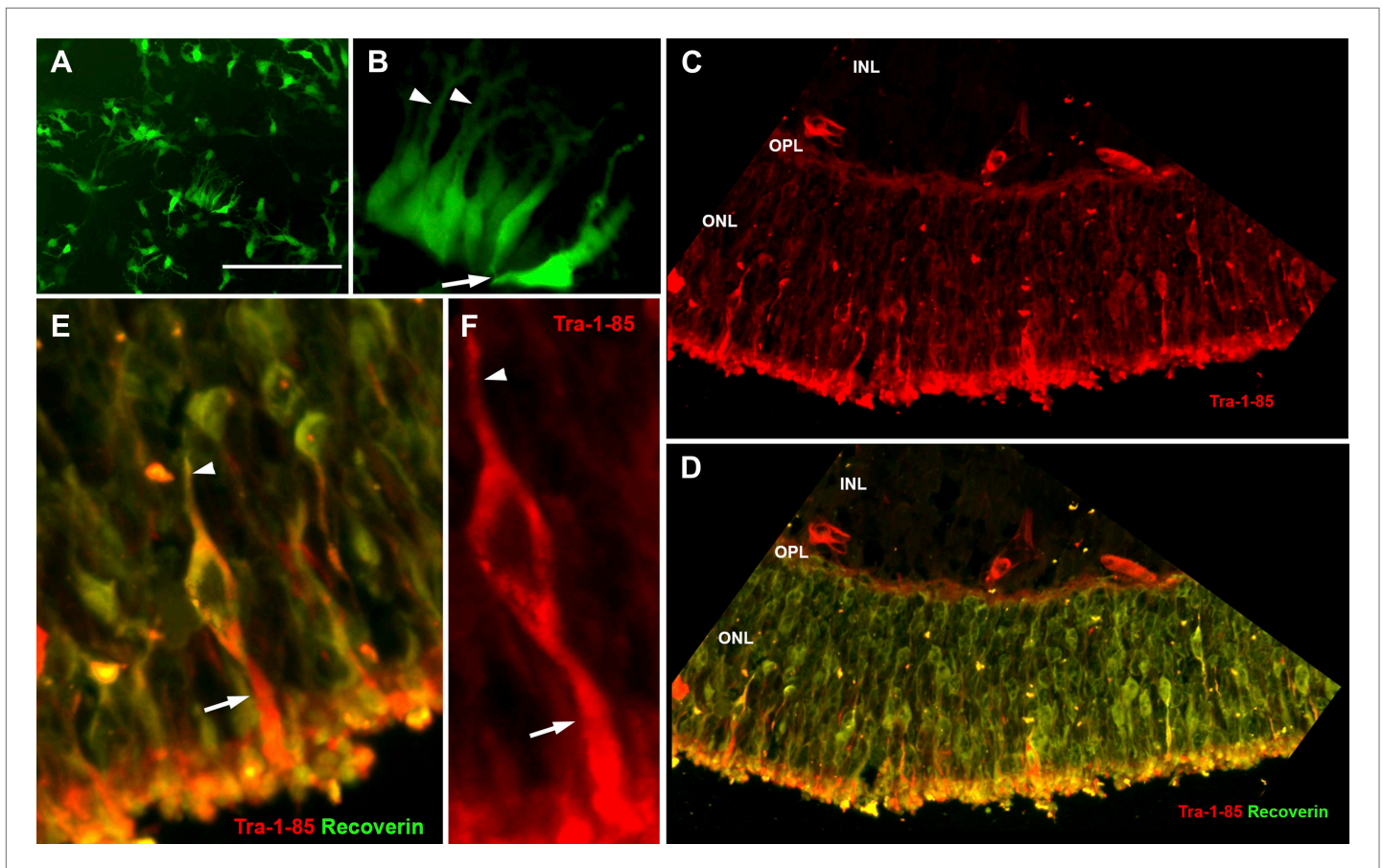
Figure 7. *USH2A*-associated photoreceptor precursor cells integrate into the dystrophic mouse retina and develop into mature photoreceptor cells. (**A** and **B**) Microscopic analysis of rhodopsin kinase GFP expression in 150-day photoreceptor precursor cells at 14 days post-plating. (**C**–**E**) Immunocytochemical analysis performed on the retinas of *Rag*$^{-/-}$ x *Crb1*$^{-/-}$ degenerative eyes 14 days after receiving subretinal injections of patient-specific photoreceptor precursor cells targeted against expression of the human cell antigen Tra-1-85 (**C**–**F**) and the photoreceptor marker recoverin (**D** and **E**). Scale bar = 50 μm.
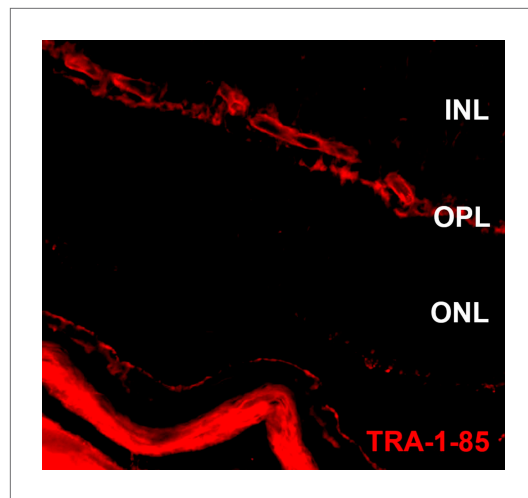DOI: 10.7554/eLife.00824.011

Figure 7—figure supplement 1. *USH2A*-associated photoreceptor precursor cells integrate into the dystrophic mouse retina. Immunocytochemical analysis performed on the *Rag*$^{-/-}$ x *Crb1*$^{-/-}$ degenerative eyes 14 days after receiving subretinal sham injections targeted against expression of the human cell antigen Tra-1-85. ONL, outer nuclear layer; OPL, outer plexiform layer; and INL, inner nuclear layer.
DOI: 10.7554/eLife.00824.012